

Quantum Theory of Solid-Liquid Coexistence and Interface in ^4He

F. Pederiva, A. Ferrante,* and S. Fantoni

*Scuola Internazionale Superiore di Studi Avanzati—International School for Advanced Studies,
Via Beirut 2/4, Trieste, Italy*

L. Reatto

*Dipartimento di Fisica, Università di Milano, Via Celoria 16, Milano, Italy
(Received 21 January 1994)*

We present a variational Monte Carlo simulation of solid-liquid coexistence and interface in ^4He at $T = 0$ K. We employ a new, generalized form of the shadow wave function in which intershadow correlations are made explicitly dependent on a local density operator. This form allows for a unique representation of the ground state for the whole range of density extending over the two phases. In the phase transition region the stable state consists of a slab of crystal coexisting with the fluid. We obtain the local density, the order parameter, and the interfacial energy for the {100} surface of an fcc crystal.

PACS numbers: 67.40.Db, 02.50.Ng, 68.45.-v

The interface between liquid and solid ^4He is a fascinating quantum object. It has unique properties [1] like melting-freezing waves and it makes possible the study of the intrinsic mechanism of crystal growth [2] which is very difficult to reach with other substances. More generally it is an example of an inhomogeneous quantum system, which is an area of strong current interest. The liquid-solid interface of ^4He is under active experimental study [2] and important theoretical results [1] and predictions have been obtained on the basis of phenomenological models. On the other hand, the problem has not been tackled by the microscopic many body theory or by quantum simulations [3,4]. Path integral methods [5], in principle, can be applied to this problem, but the difficulty lies in the large number of particles one should use in order to obtain *bona fide* representation of the two bulklike coexisting phases. The minimal requirements for a many body theory of the interface are (i) that the Bose permutation invariance between all the particles be guaranteed, (ii) that the interface can move across the system, and (iii) that the crystalline order parameter can change continuously from the solid to the liquid value. All this is completely out of reach of standard variational theory [6] in which different *functional* forms of the wave function are used for the liquid and for the solid. Moreover, for the solid phase, *a priori* equilibrium positions have to be introduced. The recently proposed shadow wave function [7] is interesting for this problem, because a unique functional form describes both the liquid and the solid phase and localization of particles only arises via interparticle correlations and no explicit breaking of the translational invariance has to be introduced. Yet the problem remains that in the shadow wave function the values of the parameters are density dependent, so that they have different values in the liquid and in the solid.

In this Letter, we present the first microscopic compu-

tation of the solid-liquid coexistence and interface in ^4He at $T = 0$, as a study of quantum effects in the freezing and melting phenomena. Our results are obtained with a variational Monte Carlo simulation based on an extension of the shadow wave function in which the correlating factors are made dependent on a local density operator. We show that in this way a unique wave function can be obtained which gives a realistic description of ^4He from the equilibrium liquid density up to high density, well inside the solid phase. In an intermediate density range two distinct phases do coexist so that we can study the interfacial region.

In the shadow wave function correlations between the atoms are represented explicitly by pair terms and implicitly via a coupling to subsidiary variables:

$$\psi(R) = e^{-\sum_{i<j} \hat{u}_{pp}(r_{ij})/2} \times \int dS e^{-\sum_i \hat{u}_{ps}(|r_i - s_i|) - \sum_{i<j} \hat{u}_{ss}(s_{ij})}, \quad (1)$$

where $R = (\mathbf{r}_1, \dots, \mathbf{r}_N)$ and $S = (\mathbf{s}_1, \dots, \mathbf{s}_N)$. In the original ansatz [7] the pseudopotentials \hat{u} are simple functions of the displayed arguments (we indicate this by taking out the hats) and, more specifically, $u_{pp}(r) = (b_p/r)^5$, $u_{ps} = Cr^2$, and $u_{ss}(r) = (b_s/r)^{m_s}$, with b_p , C , b_s , and m_s being variational parameters. Minimization of the energy gives a density dependent set of parameters. Here, we generalize the wave function by assuming that the pseudopotentials depend on the local density operator. For a particle at position \mathbf{r}_i we assume the convenient form:

$$\hat{\rho}_i = \frac{1}{A} \sum_l \{1 + \exp[\mu(r_{il} - r_c)]\}^{-1}, \quad (2)$$

where A is the normalization constant.

From previous computations [7] it is known that b_s is the parameter with the strongest density variation and that freezing is to a large extent driven by the shadow variables. In order to be as simple as possible we have assumed that only \hat{u}_{ss} depends on the local density of shadows [8] as follows:

$$\hat{u}_{ss}(s_{ij}) = \left(\frac{b_0 + b_1 \frac{\hat{\rho}_i + \hat{\rho}_j}{2}}{s_{ij}} \right)^{m_s}. \quad (3)$$

The parameters m_s , b_p , and C are taken at all densities to have their optimal values at the equilibrium density ($b_p = 1.12\sigma$, $C = 4\sigma^{-2}$, and $m_s = 9$, where $\sigma = 2.556 \text{ \AA}$). The remaining parameters are determined by the condition of a global minimization of the expectation value $\epsilon = \langle H \rangle / N$ of the energy over the density range $\rho_{\min}\sigma^3 = \rho_{\text{eq}}\sigma^3 = 0.365$ and $\rho_{\max}\sigma^3 = 0.55$. The values of μ and r_c are not crucial as long as the range of $\hat{\rho}_i$ lies in between the first two shells of neighbors. The resulting values are $b_0 = 0.51\sigma$, $b_1 = 1.91\sigma^4$, $\mu = 3\sigma^{-1}$, and $r_c = 2.1\sigma$. In the Hamiltonian H we have used the standard HFDHE Aziz potential [3].

This wave function, the local density-shadow wave function (hereafter denoted as LD-SWF), is explicitly symmetric in the particle coordinates and translationally invariant. In the presence of density fluctuations on a scale of some interatomic distances, it adjusts the parameters in a self-consistent way and it is therefore suitable to describe liquid-solid coexistence in ^4He . We have tested the LD-SWF on the homogeneous systems, and found that it reproduces almost exactly the equation of state obtained when $\hat{\rho}_i$ in Eq. (3) is replaced by the average density. When N , the number of ^4He atoms, is few hundreds, the system exhibits two different branches of the energy, a liquid and a solid one, which are present at low and high density, respectively. The obtained results are in reasonably good agreement with the optimal results of Vitiello *et al.* [7], as can be seen in Fig. 1. In this figure we also report, for the sake of comparison, the Green function Monte Carlo results of Ref. [3]. When N is large (we have considered the range 1500–4000) there exists a density interval in which there is coexistence between liquid and solid.

In this first analysis we were mostly interested in verifying the possibility of describing the liquid-solid coexistence. Therefore we have chosen a geometry as simple as possible, that is, the {100} interface of an fcc crystal. Results for other geometries will be given elsewhere. The initial configuration consists of a given number of {100} layers of the fcc crystal in the middle of a simulation box in contact with random configurations on the two sides along the z direction. Each layer of the solid accommodates 32 particles. One Monte Carlo step (MCS) consists of a sweep over all the particle and shadows degrees of freedom, and periodical boundary conditions are applied in all directions. Typical runs are of the order of 2.5×10^5 MCS, preceded by an equilibration of about 2×10^4 MCS.

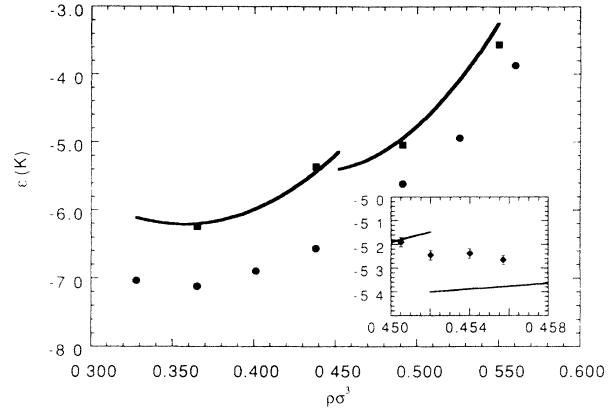


FIG. 1. Equation of state of ^4He . Solid line: LD-SWF; circles: GFMC results from Ref. [3]; squares: SWF results from Ref. [7]. The inset shows LD-SWF results in the coexistence region.

Statistical errors have been computed from the variance and the autocorrelations of the estimators.

During the simulation several physically relevant quantities have been evaluated. First of all, we have considered global estimators, like the energy of the whole sample. The inset in Fig. 1 shows the values of the energy per particle ϵ obtained in the coexistence region for several values of ρ_{av} [9].

The analysis of the interface has required the evaluation of several other estimators measuring local properties as a function of z . One is the crystalline order parameter, given by

$$O_\alpha = \left\langle \left| \frac{1}{N_\nu} \sum_{l=1}^{N_\nu} e^{i \frac{4\pi}{a} \hat{n}_\alpha \cdot \mathbf{r}_l} \right|^2 \right\rangle, \quad (4)$$

with $\alpha = x, y, z$, \hat{n}_α the corresponding vectors, N_ν the number of particles in the ν th layer, and a the side of the cubic cell. O_x , O_y , and O_z have been accumulated for each layer ν , with a layer width which has been taken equal to the {100} interlayer distance. Figure 2 reports the results for the longitudinal order parameter $O_L = O_z$ and the transverse one $O_T = (O_x + O_y)/2$. Figure 3 gives the fine scale density profile, defined as $\langle \rho(z_i) \rangle = \langle N_i \rangle / \Delta V$, where ΔV is the volume of a layer resulting from binning the box in ~ 800 bins in the z direction.

We find that when $\rho_{\text{av}}\sigma^3$ falls in the range $\rho_f\sigma^3 = 0.449 \pm 0.001$ and $\rho_m\sigma^3 = 0.456 \pm 0.002$ the stable state corresponds to an inhomogeneous situation in which part of the system has crystalline order at density ρ_m and part is disordered at density ρ_f , as can be seen in Fig. 3 [10]. The amount of the two phases depends only on ρ_{av} and is consistent with the so-called “lever rule”: $\rho_{\text{av}} = \rho_m \cos^2(\theta) + \rho_f \sin^2(\theta)$. We have verified that we are sampling an equilibrium state by starting from different initial conditions corresponding to a different amount of solid and liquid: after equilibration, the amount of solid phase is independent of the initial configuration. A closer

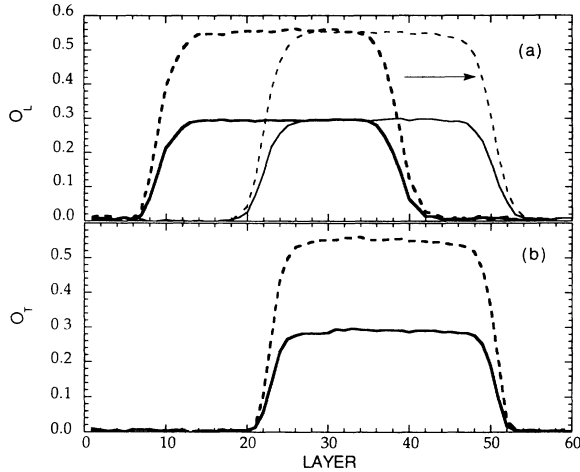


FIG. 2. Longitudinal (a) and transverse (b) order parameter as a function of layer position at $\rho\sigma^3 = 0.452$. Solid line: particles; dashed lines: shadows. The two displayed results for the longitudinal order parameter refer to different block averages along a unique MC run.

analysis of the interface can be done following the motion of the particles during the random walk. As we can see in Fig. 4, the particles well inside the solid are localized around the lattice site, even if they experience a quite large motion. Going through the interface we can observe a larger diffusivity, coming to a completely disordered situation when we look at the liquid phase. This plot shows the existence of an interfacial region 4–5 layers wide.

We find one striking difference between the present results for a quantum system and the results [11] of simulation of liquid-solid coexistence for classical particles: in the present case the interfaces between liquid and solid are very mobile. Taking block averages over 30 000 MCS we find that in a block the solid slab is located at a different position than in a successive block, and the solid can be found in a region where previously the system was liquid. An example of this is shown in Fig. 2. It is a clear evidence of the actual indistinguishability of the particles, such that each particle is likely to be found either in the liquid or the solid region. What remains essentially constant during the simulation is the ratio between the volume of solid and liquid. This mobility is absent in the case of classical particles and it is suggestive that it is a manifestation of the zero point motion of freezing-melting density waves which is captured in our small system.

Many body correlations characterize indeed the quantum systems, because the Jastrow function, which is of the pair product form, fails in the description of the solid. Many body correlations, as introduced by the shadow variables, have an essential role in allowing wide local motions of the atoms around the equilibrium positions, while long range order is maintained. There is evidence that these correlations are beyond the triplet level. In the coexistence region the variation of the local density

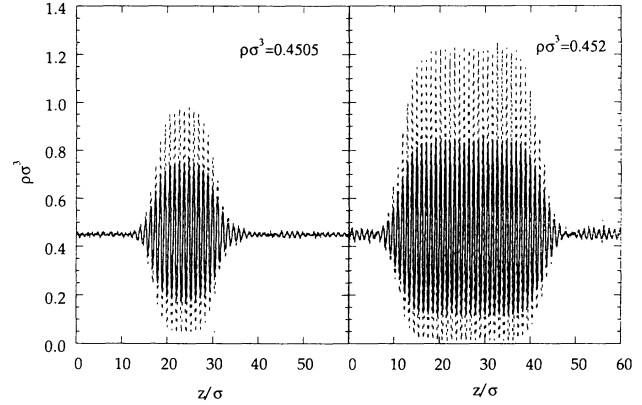


FIG. 3. Fine scale density profile at two different densities in the coexistence region. Solid line: particles; dotted line: shadows.

induces a variation of the local many body correlations which then also dominate the interface. All this is absent in the classical case where pair terms in the Boltzmann distribution function are at the origin of freezing.

We have obtained a first estimate of the liquid-solid interfacial energy by fitting the energies in the two phase region as a function of the specific volume with a linear formula:

$$\epsilon(v) = \epsilon(v_m) \cos^2 \theta + \epsilon(v_f) \sin^2 \theta + \frac{2S}{N} \sigma_{\text{int}}, \quad (5)$$

where S is the area of the x - y section, v_m and v_f are the melting and freezing specific volumes given by the calculation. The fit gives $\sigma_{\text{int}} = 0.18 \pm 0.07 \text{ K}/\text{\AA}^2$. The error is mostly due to the uncertainty on the values of the freezing and melting densities. A similar estimate is obtained by replacing $\epsilon(v_m)$ and $\epsilon(v_f)$ in Eq. (5) with the average value of the local energy evaluated, respectively,

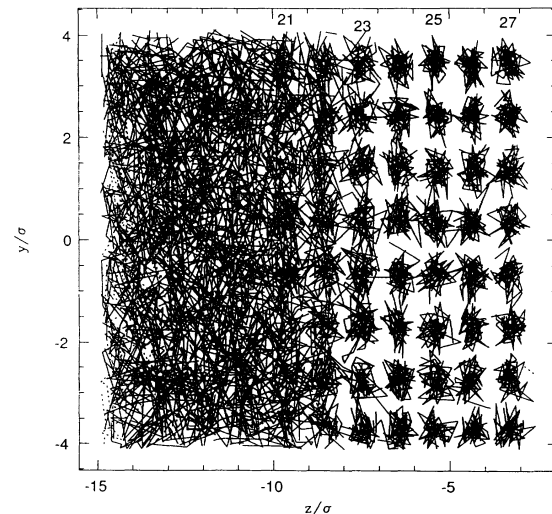


FIG. 4. Trajectory plot of particles projected on the y - z plane, for layers in the interfacial region.

in the solid and the liquid region of a two phase simulation. Our result for the interfacial energy is consistent with the value deduced from experiment [12]. However, one should keep in mind two significant differences: experiments refer to basal plane of the hcp crystal, and the temperature is not low.

The equation of state given by our LD-SWF has an anomalous behavior in the two phase region (see inset in Fig. 1). The Maxwell construction based on the energies of single phase states gives $\rho_f^M \sigma^3 = 0.407$ and $\rho_m^M \sigma^3 = 0.467$, quite different from the values 0.449 and 0.456 of the direct computation. Maxwell construction is appropriate for an infinite system so a possible source of the discrepancy is the finite size effect. We can rule out that this is important in our case because a computation with a box twice as long gives essentially the same value of $v_f - v_m$. On the other hand we have found that $v_f - v_m$ is much more sensitive than $\epsilon(v)$ on the parametrization of \hat{u}_{ss} in Eq. (3). In fact, we have been able to choose values of the coefficients b_0 and b_1 such that $v_f - v_m$ becomes substantially larger and closer to the value given by the Maxwell construction, with marginal changes in $\epsilon(v)$. Studies and simulations in classical systems indicate that larger steepness of the repulsive force [13], as well as the presence of an attractive tail [14], increases $(v_f - v_m)/v_m$. It is known [15] that a significantly better representation of the liquid phase region of ${}^4\text{He}$ is obtained if the intershadow pseudopotential u_{ss} is represented by the Aziz rescaled function. On the basis of the previous considerations its use should enlarge the two phase region in this quantum system. In any case, we have strong indications that the present results for the interfacial energy and width and for the order parameter profile will not be significantly changed by a more accurate parametrization of $u_{ss}(r)$. In fact, we find that these quantities do not change in a significant way when the values of b_0 and b_1 in Eq. (3) are changed as discussed above. This implies that such quantities are to a large extent determined by the mismatch between an ordered and a disordered phase and not so much by how large is the density discontinuity between the two phases.

In conclusion, we have shown that the study of the liquid-solid interface of a quantum system is feasible within the variational many body theory and we have provided the first microscopic estimate of the interfacial energy and width. A specific quantum effect is the high mobility of the interface, but, at the same time, the interface is quite well defined. These results are based on an extension of the shadow wave function in which interparticle correlations are introduced, which depend on the local environment of each particle. We believe that this approach can be useful in the study of many other inhomogeneous many body systems, such as a fluid close to a wall, the liquid-vacuum interface, or clusters. Some

exploratory studies [16] of clusters of ${}^4\text{He}$ atoms have already given interesting results.

We would like to thank G. V. Chester, M. H. Kalos, S. A. Vitiello, and E. Tosatti for many useful discussions. This work has been supported in part by Consorzio INFN and by Ministero dell' Università e della Ricerca Scientifica e Tecnologica.

* Present address: Fakultät für Physik, Universität Konstanz, Postfach 5560, D-78434 Konstanz, Germany.

- [1] A. Andreev, in *Excitations in 2D and 3D Quantum Fluids*, edited by A.F.G. Wyatt and H.J. Lauter (Plenum, New York, 1991), p. 397.
- [2] E. Rolley, E. Chevalier, C. Guthmann, and S. Balibar, *Phys. Rev. Lett.* **72**, 872 (1994); O.A. Andreeva, K.O. Keshishev, A.B. Kogan, and A.N. Marchenkov, *Europhys. Lett.* **19**, 683 (1992).
- [3] M.H. Kalos, M.A. Lee, P.A. Whitlock, and G.V. Chester, *Phys. Rev. B* **24**, 115 (1981).
- [4] S.A. Chin and E. Krotschek, *Phys. Rev. Lett.* **65**, 2658 (1990).
- [5] D.M. Ceperley and E.L. Pollock, *Phys. Rev. Lett.* **56**, 351 (1986).
- [6] S.A. Vitiello and K.E. Schmidt, *Phys. Rev. B* **46**, 5442 (1992); Q.N. Usmani, S. Fantoni, and V.R. Pandharipande, *Phys. Rev. B* **26**, 6123 (1982).
- [7] S.A. Vitiello, K.J. Runge, and M.H. Kalos, *Phys. Rev. Lett.* **60**, 1970 (1988); S.A. Vitiello, K.J. Runge, G.V. Chester, and M.H. Kalos, *Phys. Rev. B* **42**, 228 (1990).
- [8] One could use the density of particles. However, the path integral scheme suggests that the density of shadows is the more appropriate variable. See L. Reatto and G.L. Masserini, *Phys. Rev. B* **38**, 4516 (1988); L. Reatto, in *Recent Progress in Many-Body Theories*, edited by C.E. Campbell and E. Krotschek (Plenum, New York, 1992), p. 221.
- [9] The difference found for $\epsilon(\rho)$ approaching the melting density from the homogeneous solid and the coexistence branch is due to deformations in the grown crystal and residual interfacial effects.
- [10] Experimental values are $\rho_f \sigma^3 = 0.430$ and $\rho_m \sigma^3 = 0.468$. See P.R. Roach, J.B. Ketterson, and C.W. Woo, *Phys. Rev. A* **2**, 543 (1970).
- [11] J.N. Cape and L.V. Woodcock, *J. Chem. Phys.* **73**, 2420 (1980), and references therein.
- [12] D.O. Edwards, M.S. Pettersen, and H. Baddar, in *Excitations in 2D and 3D Quantum Fluids* (Ref. [1]), p. 361.
- [13] W.G. Hoover, S.G. Gray, and K.W. Johnson, *J. Chem. Phys.* **55**, 1128 (1971).
- [14] R.J. Galejs, H.J. Raveche, and G. Lie, *Phys. Rev. A* **39**, 2574 (1989).
- [15] T. MacFarland, S.A. Vitiello, and L. Reatto, *J. Low Temp. Phys.* **89**, 433 (1992).
- [16] S. Zhang, M.H. Kalos, G.V. Chester, S.A. Vitiello, and L. Reatto, *Physica (Amsterdam) A* (to be published).

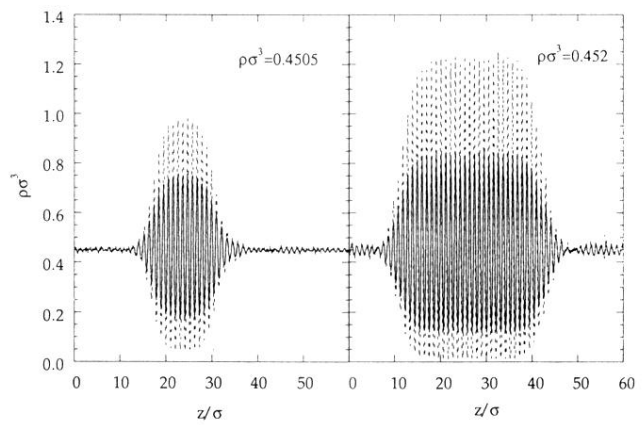


FIG. 3. Fine scale density profile at two different densities in the coexistence region. Solid line: particles; dotted line: shadows.

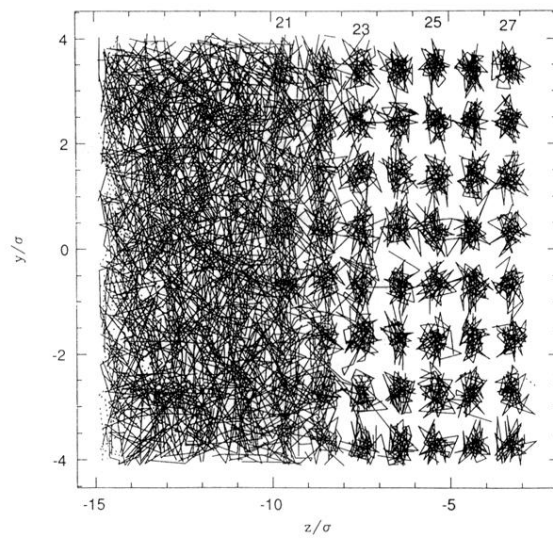


FIG. 4. Trajectory plot of particles projected on the y - z plane, for layers in the interfacial region.